Available online at www.sciencedirect.com
SCIENCE DIRECT®
Polymer 44 (2003) 4011–4019
polymer
www.elsevier.com/locate/polymer

Wet spinning of low gel content SBR/PMMA core/shell particles dispersed in a good solvent for the shell

M.R. Moghbeli[a], N. Mohammadi[a,*], R. Bagheri[b], S.R. Ghaffarian[a]

[a]*Loghman Fundamental Research Group, Department of Polymer Engineering, Amirkabir University of Technology, P.O. Box 15875-4413, Tehran, Iran*
[b]*Department of Materials Science and Engineering, Sharif University of Technology, P.O. Box 11365-9466, Tehran, Iran*

Received 21 May 2002; received in revised form 20 November 2002; accepted 10 January 2003

Abstract

A low gel content poly (styrene-*ran*-butadiene)/poly (methyl methacrylate) (SBR/PMMA) core/shell particles dispersed in a good solvent for the shell was wet spun into a coagulation bath at room temperature. The SEM micrographs of as spun fibers showed various surface topographies and fiber diameters, ranging from 4.2 up to 20 μm depend upon the draw ratio. The osmium tetroxide stained cross-section of fibers observed by transmission electron microscope (TEM), indicated a heterogeneous morphology consisting of dark cores and fairly light shells, which is a result of self-stratification to an overall core/shell morphology in fiber cross-section. The inner core consisted of higher concentration of copolymers with double bonds, while the outer shell is made mainly of ungrafted PMMA chains. The equilibrium thermodynamic analysis based on minimization of surface free energy predicts a predominant core/shell structure which the SBR chains are encapsulated mainly by ungrafted PMMA homopolymers and SBR-*g*-PMMA copolymers which agrees quite well with the observed morphology.

Keywords: Wet spinning; Core/shell particles; Stratification

1. Introduction

The preparation of fibers with a variety of functions and diverse properties, has attracted the interest of scientists for many years. Spinning of crystalline materials, e.g. proteins, starches, liquid crystals, as single components and polyblends is followed to get the high-performance fibers and composite materials [1–3]. On the other hand, spinning of amorphous polymer blends is performed to get toughend or surface-sensitive fibers.

In addition to fibers, many investigations have been conducted on thin films to study phase separation of polymer blends and figure out their surface-enrichment phenomenon [4–9]. The surface enriched structures can be used in many applications dealing with adhesion, wettability, friction, bio-compatibility, weathering, etc. This phenomenon depends on film thickness, boundary conditions, molecular weight and degree of crystallinity of the components, their surface energy difference, and the interaction between polymer components [5,6,9–12].

In surface coatings, self-stratification of two resins or polymers dissolved in a common solvent during its evaporation may end up to a desired bi-layer structure [9,13]. The results of three decades of research show that the rate of solvent evaporation, surface free energy difference between two polymer components, pigment size and its surface property, and the surface properties of substrate as important factors which affect the extent of self-stratification of the coating [13–16].

Therefore, the driving force for surface enrichment of certain component in a multi-component polymer is mainly the minimization of surface free energy of the system. In other words, the tendency of formation of a structure with a gradient composition from surface to bulk can be attributed to the tendency of the system to put the lower-surface-energy component at the surface, which causes the decrement of the Gibbs free energy of the system. Recently, Duan et al. [5] introduced another effective and crucial parameter in surface enrichment phenomenon, which is the thermodynamic interaction of the components. They prepared a series of polymer blends with various extent of hydrogen-bonding capability among the components, while showing the same surface free energy. They concluded that by increasing the extent of hydrogen bonding, the surface enrichment decreases and a more homogeneous surface of polymer blend will form.

* Corresponding author. Tel./fax: +98-21-6468243.
E-mail address: mohamadi@aut.ac.ir (N. Mohammadi).

0032-3861/03/$ - see front matter © 2003 Published by Elsevier Science Ltd.
doi:10.1016/S0032-3861(03)00055-7

Although, many investigations have been done on phase separation phenomena in thin films of polymer blends, less attention has been paid to its occurence during wet spinning of fibers. Xiao et al. [17] reported the spinnability of block copolymer micelles, poly (vinylalcohol-*b*-acrylonitrile), in a selective solvent, i.e. water. They showed that the micellar structure characteristics of the block copolymer are the key factor affecting the spinnability and surface properties of the fiber.

On the other hand, the synthesis of core/shell particles to be used as impact modifiers has been a prime interest of many scientists and companies for several decades [18–21]. It is well established that rubbery core/glassy shell particle dispersions as connected network in a brittle matrix polymer can increase its impact resistant considerably [22]. Therefore, there are some interests on the performance of artificially made core/shell particle aggregates, in a matrix.

In this research, wet spinning of structural particles, SBR/PMMA core/shell with low gel content, dispersed in a good solvent for the shell is considered. The prepared core/shell fibers can be used in different applications including fibrillar toughener in plastic matrices, which can be a new concept in polymer blends.

2. Experimental

2.1. Materials

The SBR latex, SBR 1152 (23% styrene) from NIPC Co., Iran, was used as core material to synthesize a core/shell latex via seeded emulsion polymerization technique. This selected SBR latex with low gel content is prepared under cold emulsion polymerization process. For the shell material, methyl metacrylate monomer (MMA), from Merck Co., was used after removing its inhibitor by vacuum distillation. Potassium persulfate (KPS) and sodium luryl sulfate (SLS) from Merck Co. were also incorporated without any purification. All solvents including methyl ethyl ketone, MEK, acetone, petroleum ether (boiling point about 40 °C), carbon tetrachloride were all analytical grade, Merck Co., and consumed as received. The double distilled water was prepared in the lab.

2.2. Synthesis of core/shell latices

Commercial SBR latex was filtered and used in seeded emulsion polymerization [23]. Then, the SBR particles were swelled by MMA monomer at 1/1 ratio for 16 h via tumbling at 60 rpm. The seeded emulsion polymerization was preformed in a tumbling reactor at 65 °C and 40 rpm for 4 h.

2.3. Morphology of core/shell particles

Transmission Electron Microscope, TEM, Zeiss CEM 902A, was used to observe the morphology of synthetic core/shell particles. The samples were prepared on copper grid, and selectively stained by osmium tetroxide, OsO_4, in order to distinguish the core from the shell.

2.4. Particle size and size distribution

The particle size and size distribution of the seed and core/shell latex were measured via laser light scattering (Photon Correlation Spectroscopy), SEM-633, with wavelength 632.8 nm and laser source light He and Ne gas (Table 1).

2.5. Gel content and grafting degree

The gel content of SBR core was gravimetrically measured by solvent extraction. Thus, 0.25 g of dried SBR latex was dissolved in 25 g of toluene and stirred at 300 rpm for 48 h. The solution was then centrifuged at 5000 rpm at room temperature. By drying and measuring sediment phase, the gel content was determined. A similar method was used to measure the grafting degree of core/shell particles. The core/shell latex was freeze-dried and the extracted fine powder was dispersed in a good solvent for 48 h at 300 rpm at room temperature. The final dispersion was centrifuged at 5000 rpm and the resultant dope was divided to supernatant and sediment phases. By measurement of the ungrafted PMMA the grafting density was determined.

2.6. Characterization of core/shell particles by FTIR

The characterization of sol phase of core/shell particles, which were dispersed and centrifuged in a good solvent for shell, was performed by FTIR (Perkin–Elmer FTIR 1710).

2.7. Thermogravimetric analysis (TGA)

In order to determine the composition of spinning dope solutions, thermogravimetric analysis (TGA) technique (Perkin–Elmer TGA-7 model) was used. The samples were heated from 100 to 700 °C at a heating rate of 10 °C/min in nitrogen atmosphere.

Table 1
The characterizations of SBR seed and synthesized core/shell particles

Material	Gel content (%)	Size (nm)	PDI	Grafting degree[a] (%)
SBR Seed	1.5	75	1.12	–
Core/Shell (SBR/PMMA)	–	95	1.07	58.2

[a] The grafting density was measured at 1 wt% of core/shell dispersion in acetone, which stirred at 300 rpm and room temperature for 48 h.

2.8. Preparation of spinning dope and fiber formation

The freeze-dried core/shell powder was dispersed in a good solvent for shell, i. e. methyl ethyl ketone, MEK. The 5% MEK solutions were filtered before spinning and transferred into a glass injector and extruded from its 0.2 mm diameter spinneret, at a rate of 1–2.5 m/min into various non-solvent baths. The coagulating agents: water, carbon tetrachloride and petroleum ether have a wide spectrum of solubility parameters. The spinnability of dope was good in petroleum ether bath and a continuous filament was formed and were drawn to various lengths. On the other hand, the spinnability was found poor in both water and carbon tetrachloride baths, so that the formation of a continuous filament was almost impossible.

During wet spinning, the top of the spinneret was immersed into the coagulation bath. The coagulating length of the extrudates in the bath was 15 cm and after leaving from the bath, the fibers were drawn to various degrees. Finally, the samples were dried at room temperature under vacuum for 2 h.

2.9. Morphology of fibers

The longitudinal and cross-sectional surface morphology of as-spun fibers were investigated by scanning electron microscopy (SEM), Cambridge, and TEM, Zeiss CEM 902 A, respectively. The fiber samples were stuck on the SEM sample holder by a double stick tape and gold sputtered before examination. In order to observe the cross-sectional surface morphology, the fibers were molded in an epoxy resin and microtomed to a thin section. Then, the thin section was stained by osmium tetroxide in order to increase the resolution for distinguishing the various phases.

3. Results and discussion

The charateristics of the SBR seed and synthesized SBR/PMMA core/shell latices were presented in Table 1. Also, TEM micrograph shows the morphology of the nano particles, 95 nm, which have been used to prepare the spinning dope (Fig. 1).

Fig. 2 shows the longitudinal surface morphology of as extruded fibers. The undrawn fiber has a rough surface with 21.4 μm in diameter. As the draw ratio, the ratio of the final length of the drawn sample to its original length, increases from one to five, the diameter of fibers decreases and their surface becomes smoother, Fig. 2(a)–(d). The reduction of the diameter of the fibers with increasing the draw ratio can be attributed to chain orientation, while the smoothness of the surface of fibers at higher draw ratio depends on the possibility of cavity healing which is filled by solvent and non solvent in coagulation bath.

The morphology of the cross-section of as-spun fiber studied by TEM illustrates a heterogeneous structure of a

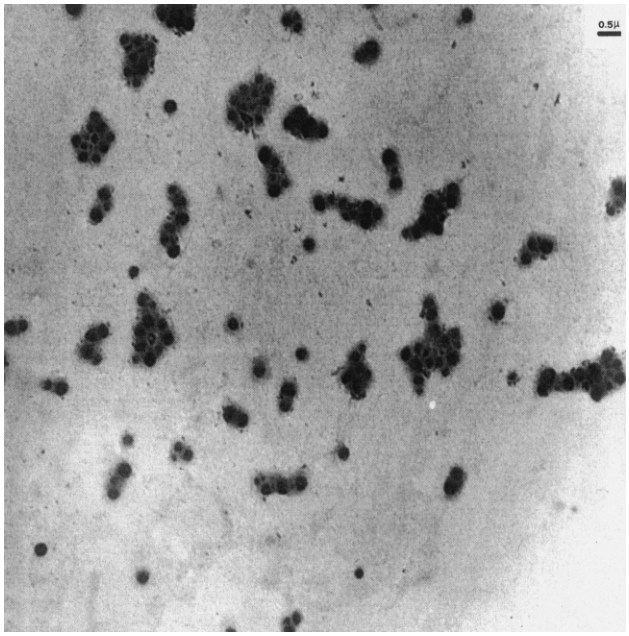

Fig. 1. TEM micrograph of synthesized SBR/PMMA core/shell particles. The sample is stained by osmiume tetroxide prior to microscopy.

dark core and a fairly light shell (Fig. 3). On the other hand, a spinodal decomposition kind of phase separation of the incompatible polymers was observed within the core and shell regions of the as-spun fibers (Fig. 4). The connectivity of dark and white regions in close observation, higher magnification, of core and shell regions in Fig. 4(a) and (b) is the main reason for this postulation. Eventhough, the thickness of the connected dark and bright regions peculiarly appear lower than the size of the original core/shell latex particle, it can be rationalized based on destruction of the structure of the original core/shell particles and their reformation during the dope preparation, its spinning and coagulation. Therefore, it seems that the heterogeneous morphology of the cross-section can be attributed to the higher concentrations of SBR or SBR grafted PMMA, SBR-*g*-PMMA, within the core region in comparison to the main localization of ungrafted PMMA homopolymer, ug-PMMA, in the shell region. The molecular weight of the SBR core is about 10^5 g/mol. On the other hand, the molecular weight of the ungrafted PMMA and grafted PMMA chains on SBR are estimated to be about 5×10^4 g/mol. The observed morphology may be interpreted based on the structure of spinning dope and morphology development of polymeric components during spinning and drying of the extrudates. Thus, a main objective of the current research has been the prediction of the observed morphology based on the minimization of the free energy of the dispersed system in coagulation bath and its stabilization during the drying stage.

First of all, it seems that by diffusion of the solvent molecules into the low gel content core/shell particles, the ug-PMMA chains diffuse into the solvent, and become solubilized and later on SBR-*g*-PMMA chains do the same

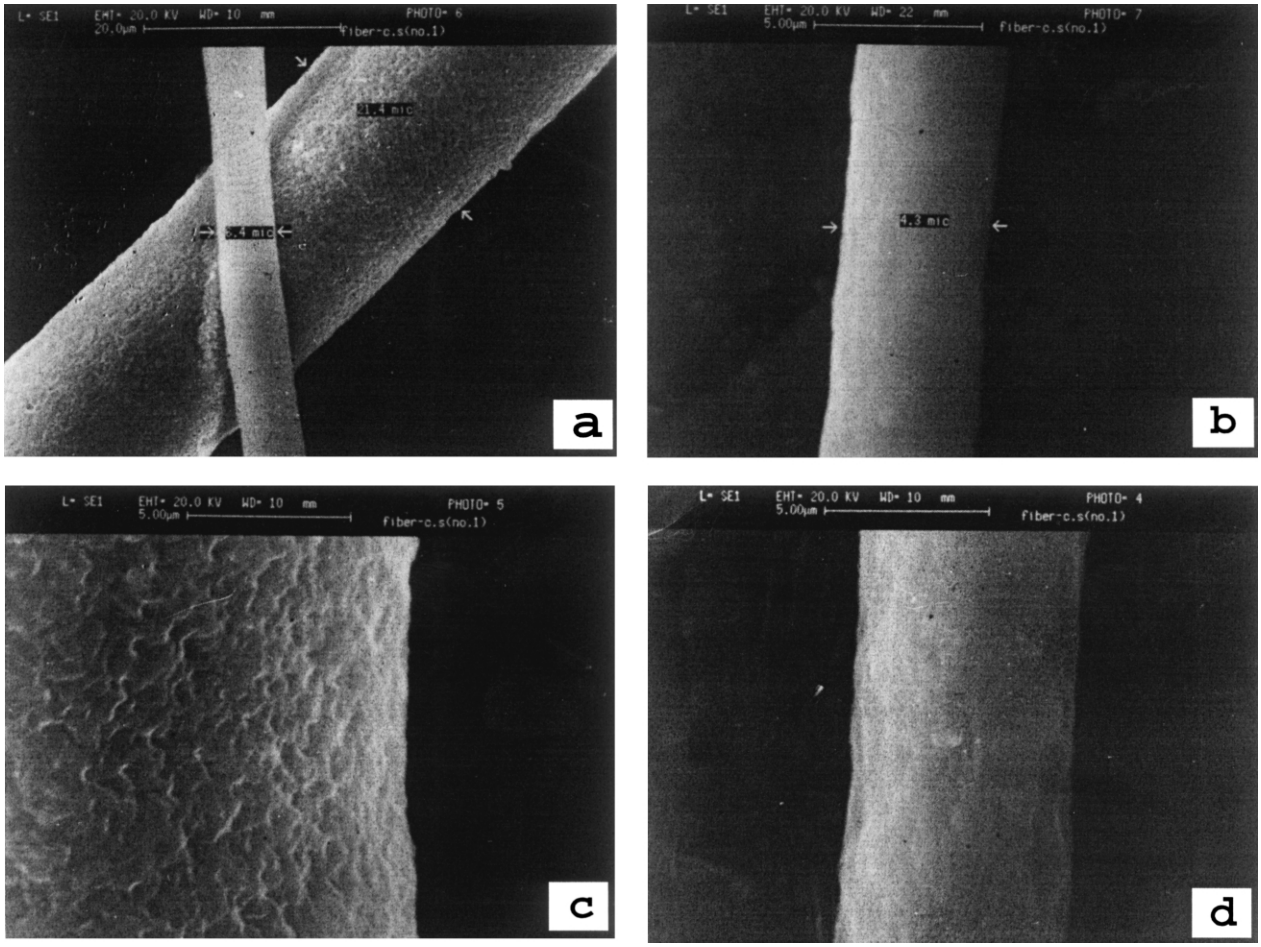

Fig. 2. SEM micrographs of as-spun fiber, (a) an undrawn and a drawn fiber with 21.4 and 6.4 μm in diameter, respectively, (b) a drawn fiber with 4.2 μm in diameter; and surface topography of fibers are seen of higher magnification, (c) Ø 21.4 μm, and (d) Ø 6.4 μm in diameter.

(Fig. 5). Interestingly, by storing the dispersions for two weeks, a fairly clear solution, without any sediment gel, could be observed (Fig. 6). This can be attributed to the formation of a heterogeneous or micro-capsulated polymeric particles consisting of SBR chains engulfed by other components in dope due to their higher tendency towards solvent media compared to SBR copolymer.

The morphological development of polymeric micelles

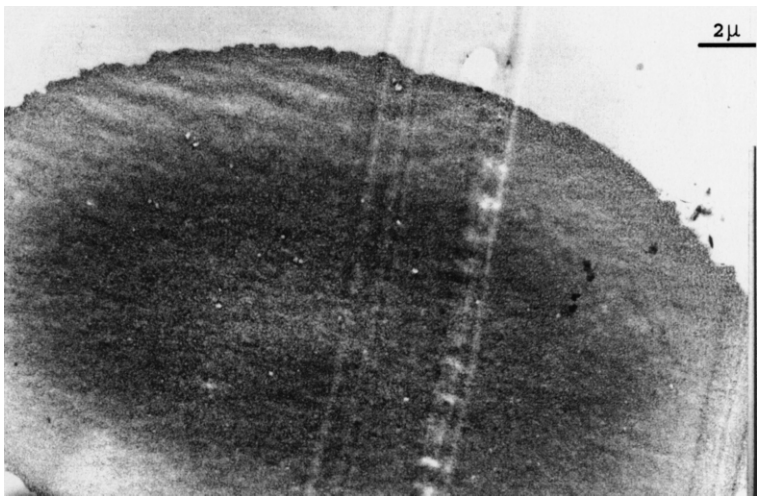

Fig. 3. TEM micrograph shows the fiber cross-section. The self-stratified morphology composed of a dark core engulfed by a fairly bright shell. The microtomed sample was stained by osmium tetroxide prior to microscopy.

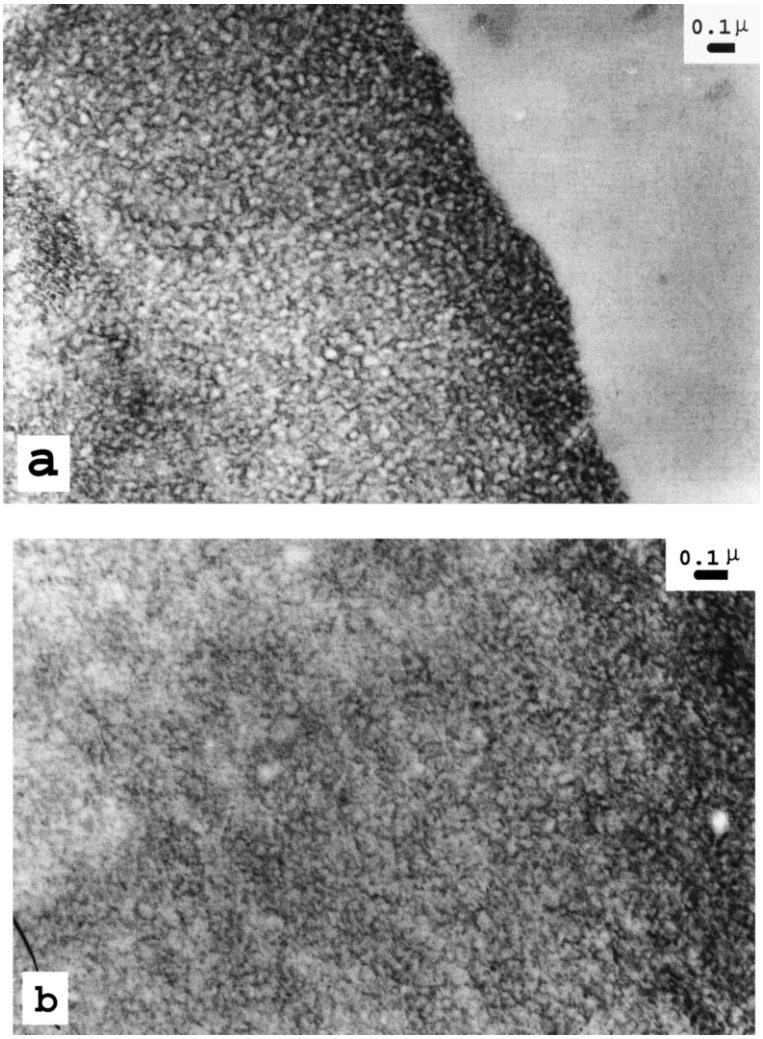

Fig. 4. The spinodal kind phase separation is seen in the cross section of the fiber in both, (a) the shell and (b) the core regions. The microtomed sample was stained by osmium tetroxide prior to microscopy.

in dope solution can be predicted using a thermodynamic analysis proposed by Sundberg et al. [24] and Chen et al. [25]:

$$\Delta G = \sum \gamma_{ij} A_{ij} - \sum \gamma_{ij}^{o} A_{ij}^{o} \quad (1)$$

Where ΔG is the change of free energy; γ_{ij} is the interfacial tension of components i and j, and A_{ij} is the corresponding interfacial area. Also γ_{ij}^{o} and A_{ij}^{o} are the primary interfacial and corresponding interfacial area, respectively. A mathematical model based on the above concept, was derived by Chen et al. [25] which gives the capability to predict the free energy changes per unit area, $\Delta\Psi = \Delta G/A$, corresponding to various morphologies in composite particles dispersed in water. Although, they modeled the morphology changes of swollen polymer particles by a monomer during the second step of emulsion polymerization, this work is focused on the application of their model to core/shell particles dispersed in a solvent. Therefore, the surface free energy and the interfacial tension of polymer pairs in the presence of a solvent will be considered.

Carr et al. [13] proposed a thermodynamic model to investigate the self-stratification behavior of two resins dissolved in a common solvent by its evaporation. Thus, they used a relation to calculate surface free energy of polymers in solvents as follow [13]:

$$\gamma^{*} = \gamma_{sol} + A\, e^{Bf} \quad (2)$$

Where γ^{*} and γ_{sol} are the surface tension of the polymer solution and the solvent, respectively. The variable f is weight fraction of the polymer, while A and B are constants and can be obtained experimentally.

The Carr's model suggests two conditions for self-stratification of a thin film containing two polymers in a solvent on a solid substrate, (i) the spontaneous wetting of the substrate by one of them, and (ii) attaining the lowest total Gibbs free energy per unit area by the required layer structure.

Therefore, the concept of the aforementioned model was applied to interpret the partial self-stratification of the as-spun fibers composed of different micellar blends (Fig. 3).

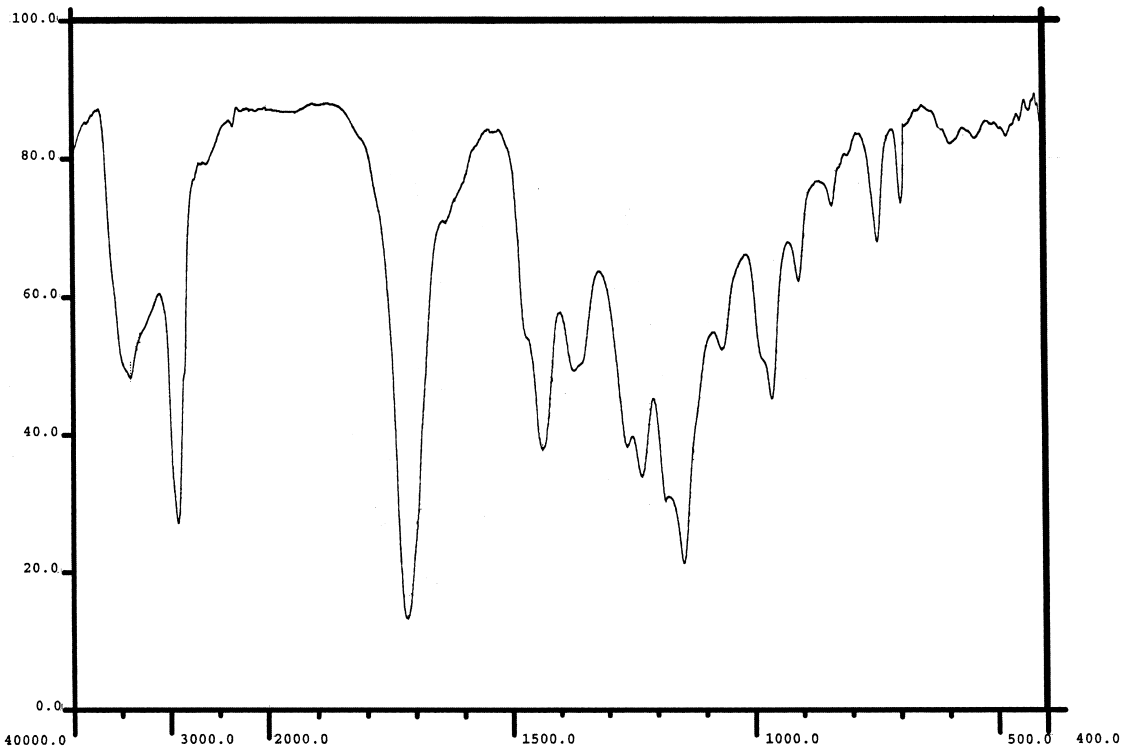

Fig. 5. FTIR spectrum of the sol phase of dispersed core/shell particles in acetone after stirring for 48 h. The wavenumber 1717 cm^{-1} corresponds to PMMA chains, while 1437, 1370, 963, and 696 cm^{-1} correspond to SBR chains.

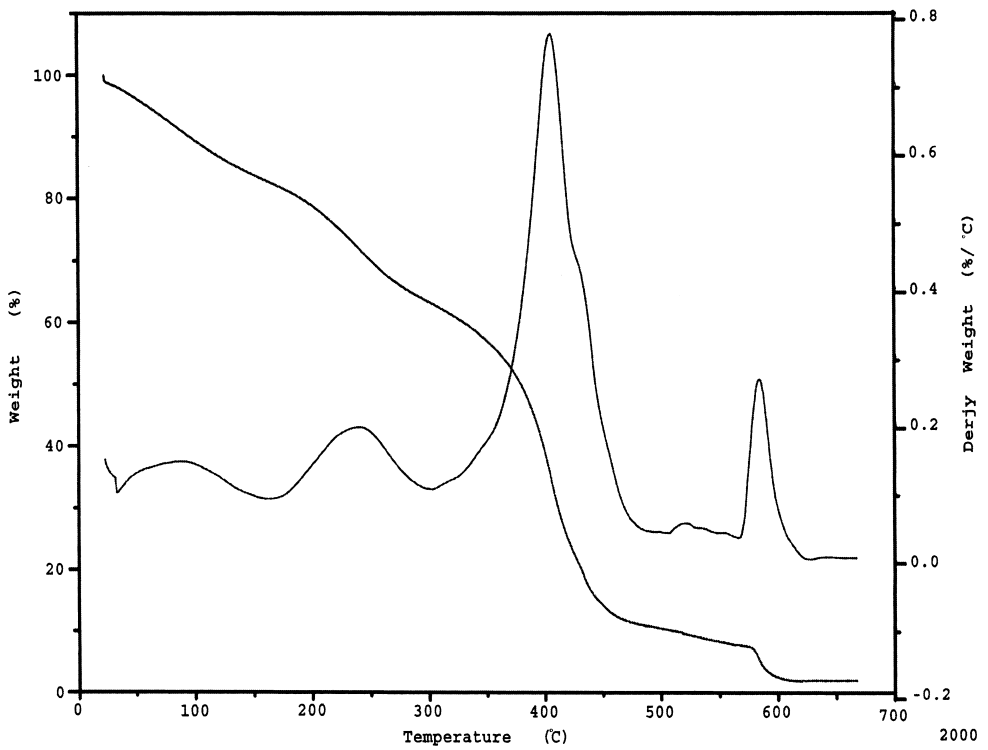

Fig. 6. TGA spectrum of the spinning dope indicates the presence of PMMA, SBR, and SBR-*g*-PMMA chains at decomposition temperatures of 270, 380, and 450 °C, respectively.

It's a special situation without any substrate involved and appears in the form of an extrudate filament. Consequently, it is necessary to make some simplified assumptions. The concentration of polymer components in the dope was assumed the same as their weight fraction in each separate layer. On the other hand, there is a very thin layer of solvent on the as-spun fiber, which desorbs or evaporates during spinning or drying, especially in low or intermediate dope concentrations. In other words, the solvent gradient throughout the fiber cross-section can be considered negligible.

Since separation of polymeric components in the spinning dope: SBR, SBR-*g*-PMMA, and ug-PMMA, for measurement of the surface tension of solution of each component in various concentration was difficult, a simple linear equation was used as a rough estimation:

$$\gamma^* = \gamma_{sol} + C.f \tag{3}$$

Where C is a constant. Furthermore, Carr's results demonstrated a negative deviation from mixture law for their systems. Thus, Chen's main equations [25] were rewritten based on the replacement of water by a solvent in order to predict the various morphological structures of polymeric micelles and colloids in a solvent media. In the following equations polymer i forms the core and polymer j is the shell layer, which engulfs the core [25]:

$$\text{Core/shell} \qquad \Delta\Psi = (\gamma^*_{ij} - \gamma_{is})(V_r + 1)^{-2/3} + \gamma_{js} \tag{4}$$

Inverted core/shell

$$\Delta\Psi = (\gamma^*_{ij} - \gamma_{is}V_r^{-2/3})(V_r^{-1} + 1)^{-2/3} + \gamma_{js} \tag{5}$$

$$\text{Individual particles} \qquad \Delta\Psi = \gamma_{js}(V_r + 1)^{-2/3}V_r^{2/3} \tag{6}$$

The core/shell particles which would be destroyed and reformed during spinning and coagulation process are substituted in Chen's equations in place of latex particles. Where γ^*_{ij} is the interfacial tension of two polymeric components in the presence of solvent, γ_{is} and γ_{js} are interfacial tension of two polymers and solvent. V_r is the volume ratio of the shell to the core and equals to $(R/R_c)^3 - 1$. R_c is the radius of the core, polymer i, and R is the overall particle diameter. In this case, $R_c = R_i$ and $R = R_j$. Hence, the aforementioned approach was applied to determine the morphology of particles made of SBR, SBR-*g*-PMMA, and ug-PMMA chains in MEK media.

The solution surface tension and interfacial tension of the polymer components with various concentrations in MEK were calculated by using Eq. (3), the Harmonic mean method, and existing literature data (Table 2). The free energy changes per unit area, $\Delta\Psi = \Delta G/A$, of the particles with different morphologies were calculated. The results show that the predominate morphology should be composed of SBR and grafted SBR core which is engulfed by ug-PMMA as core/shell particles, because this structure showed the minimum normalized free energy change in the various concentrations of polymeric particles (Table 3).

Table 2
The surface free energy of polymers and interfacial tensions between polymeric components and dope solvent, MEK

Component	Surface tension[a] (dyne/cm)			Interfacial tension[b] (dyne/cm) γ_{ij}
	γ	γ^d	γ^p	
PMMA	41.10	30.82	10.28	
SBR	30.00	29.50	0.50	
SBR-*g*-PMMA	37.67	30.42	7.25	
PMMA/SBR				8.89
PMMA/SBR-*g*-PMMA				0.51
SBR/SBR-*g*-PMMA				5.90
PMMA/MEK				8.35
SBR/MEK				18.37
SBR-*g*-PMMA/MEK				10.64

[a] Refs. [26,27].
[b] Calculated based on the Harmonic mean method and literature data on surface free energy and its dispersive and polar components [26,28].

After spinning into coagulation bath, petroleum ether, the dissolved polymeric components of the dope coagulate as a filament. The coagulating agent solidifies the outer layer of extrudate faster than the inner layers because it contacts the non-solvent first. Therefore, the rough surface of the undrawn extrudate shows the instantaneously collapsed polymeric chains on the fiber surface.

The predominant morphologies of the particles in dope are predicted to be the encapsulated SBR with ug-PMMA homopolymer and SBR-*g*-PMMA copolymer up to 70% dope concentration (Table 3). Beyond 70% concentration, and obviously somewhere before solid coagulate state of core/shell particles the SBR-*g*-PMMA copolymer show more tendency to cover the SBR than the ug-PMMA. Accordingly, it can be assumed that the dope is mainly composed of a blend of SBR/PMMA and SBR/SBR-*g*-PMMA core/shell particles. Therefore, three kinds of particles can be thought within the extrudate filament: (i) SBR/PMMA composite particles form the outer layer while SBR/SBR-*g*-PMMA micelles locate in the core, (ii) the reverse of scenario i, and (iii) a homogeneous blend of both kind of particles form the surface and the bulk of the fiber, based on their weight fractions in the dope. The conditions for the self-stratification of dispersed colloids in the solvent, and extruded filament, are as follow:

$$\gamma^*_{ij} \geq 0 \tag{7}$$

$$\gamma^*_{ij} > \gamma^*_j \tag{8}$$

$$\gamma^*_i > \gamma^*_j \tag{9}$$

Where γ^*_i and γ^*_j are solution surface energies of components i and j, respectively. While γ^*_{ij} is interfacial tension of components i and j in solution. Under above conditions, the components j and i form outer and inner layers of as-spun filament, respectively. Accurate data of

Table 3
Free energy changes per unit area for micelles with various morphological structures in MEK at different solid concentrations

Morphology	$\Delta\Psi$ (erg/cm^2)		
	SBR/PMMA	SBR/SBR-*g*-PMMA	SBR-*g*-PMMA/PMMA
Dope Con. 10%			
Core/shell	0.26	2.56	3.67
Inverted core/shell	10.37	10.36	5.99
Individual particles	6.16	7.87	6.18
Dope Con. 20%			
Core/shell	0.34	2.50	3.68
Inverted core/shell	10.48	10.42	6.02
Individual particles	6.16	7.87	6.18
Dope Con. 50%			
Core/shell	0.83	2.86	3.72
Inverted core/shell	11.34	10.86	6.07
Individual particles	6.16	7.87	6.18
Dope Con. 70%			
Core/shell	1.63	3.31	3.77
Inverted core/shell	12.66	11.62	6.16
Individual particles	6.16	7.87	6.18
Solid			
Core/shell	4.18	5.15	3.89
Inverted core/shell	16.93	14.72	6.37
Individual particles	6.16	7.87	6.18

The volume ratio, V_r, was assumed equal one which was calculated based on the original diameters of the core/shell and core particles.

surface tension of polymer solution as a function of its concentration is necessary to predict the correct morphology of the final fiber. In low and intermediate dope concentrations, it is evident that the above conditions are satisfied due to the difference between the interfacial tension of PMMA-MEK pair, $\gamma^*_{PMMA/MEK} = 8.35$ dyne/cm and SBR-*g*-PMMA/MEK pair, $\gamma_{SBR\text{-}g\text{-}PMMA/MEK} = 10.64$ dyne/cm. At least, based on an enthalpic view these values show stronger interaction between PMMA and MEK, compared to SBR-*g*-PMMA. So outer layer containing higher amount of SBR/PMMA core/shell micelles by virtue of self-stratifying phenomena will cover the layer containing higher amount of SBR/SBR-*g*-PMMA composite micelles. At the high dope concentration, the situation will be changed due to higher surface free energy of solid PMMA than that of solid SBR-*g*-PMMA (Table 2). However, some resistant forces, kinetic barriers, can stabilize the preformed arrangement of stratified layers and postpone any further perturbations in high solid concentrations. The high viscosity of dope within the as-spun fiber, the uprising of ug-PMMA glass transition due to evaporation of MEK, and consequently the decrease in mobility of PMMA segments can cause the above limitations. Thus, the specific cross-sectional morphology of as-spun fiber consists of a dark core region involving more stained SBR and grafted SBR copolymer chains and a fairly light shell involving un-stainable ug-PMMA chains (Fig. 3). In both regions, core and shell, the phase separation between incompatible components, SBR and PMMA, takes place while the solvent evaporates.

4. Conclusion

The structure of core/shell particles with low gel content, dispersed in acetone, broke up to their original molecular components including soluble grafted copolymer, SBR-*g*-PMMA, ug-PMMA, and insoluble SBR copolymers in the acetone or dope solvent, MEK. The thermodynamic analysis predicted a predominant core/shell structure for micellar colloids in which the SBR chains are engulfed mainly by ug-PMMA homopolymer and SBR-*g*-PMMA copolymer within the spinning dope. The spinning of solution into a suitable coagulating bath has produced as-spun fibers with considerable drawability. The cross-sectional surface of as-spun fiber shows partially stratified morphologies composed of a stained dark core and fairly light shell regions. The inner core involved higher concenteration of copolymers with double bonds, such as SBR-*g*-PMMA and SBR and less amount of ug-PMMA compared to the outer shell. All these new morphological features are controlled by the tendency of systems toward minimizing their surface free energies. Relatively good agreement is found between the prediction of some thermodynamic models and the structures observed.

References

[1] Arcidiacono S, Mello CM, Butler M, Welsh E, Soares JW, Allen A, Ziegler D, Laue T, Chase S. Macromolecules 2002;35:1262–6.

[2] Buehler F, Baron V, Schmid E, Meier P, Schultze HJ. US Patent 5516815, 1996.
[3] Gilbert RD, Hu X, Fornes RE. J Appl Polym Sci 1995;58:1365–70.
[4] Budkowski A. Adv Polym Sci 1999;148:1–111.
[5] Duan Y, Pearace EM, Kwei TK, Hu X, Rafailovich M, Sokolov J, Zhou K, Schwarz S. Macromolecules 2001;34:6761–7.
[6] Tanaka K, Takahara A, Kajiyama T. Macromolecules 1999;29: 3233–8.
[7] Karim A, Slawecki TM, Kumar SK, Douglas JF, Satija SK, Han CC, Russell TP, Liu Y, Overney R, Sokolov J, Rafailovich M. Macromolecules 1998;31:857–62.
[8] Dalnoki-Veress K, Forrest JA, Stevens JR, Dutcher JR. J Polym Sci, Part B: Polym Phys 1996;34:3017–24.
[9] Geoghegan M, Jones RAL, Payne RS, Sakellarion P, Clough AS, Penfold J. Polymer 1994;35:2019–27.
[10] Wendlandt M, Kerle T, Heuberger M, Klien J. J Polym Sci, Part B: Polym Phys 2000;38:831–7.
[11] Kumar SK, Weinhnold JD. Phys Rev Lett 1996;77:1512–5.
[12] Omaraee IA, Mohammadi N. Polym Eng Sci 2003;42:2328–35.
[13] Carr C, Wallstom E. Prog Org Coat 1996;28:161–71.
[14] Joly M. Prog Org Chem 1995;28:486–95.
[15] Funke W. Prog Org Coat 1974;2:289–98.
[16] Vink P, Bots TL. Prog Org Coat 1996;28:173–81.
[17] Xiao W, Xu X, Chen K. Polym Eng Sci 1994;34:975–80.
[18] Paul DR, Bucknall CB. Polymer blends. Performance, vol. 2. New York: Wiley; 2000. p. 137.
[19] Cho K, Yang JH, Park CE. Polymer 1997;28:5161–7.
[20] Lombardo BS, Kesskkula H, Paul DR. J Appl Polym Sci 1994;54: 1697–720.
[21] Lu M, Kesskkula H, Paul DR. J Appl Polym Sci 1996;59:1467–77.
[22] Qian JY, Pearson RA, Dimonie VL, Shaffer OL, El-Aasser MS. Polymer 1997;38:21–30.
[23] Moghbeli MR, Mohammadi N, Bagheri R. Submitted for publication.
[24] Sundberg DC, Casassa AP, Pantazopouos J, Muscato MR. J Appl Polym Sci 1990;41:1425–42.
[25] Chen Y, Dimonie V, El-Aasser MS. J Appl Polym Sci 1991;42: 1049–63.
[26] Wu S. Polymer interface and adhesion. New York: Marcel Dekker; 1982. p. 180.
[27] Zallat MF, Nardin M. J Adhes 1996;57:115–31.
[28] Whim BP, Johanson PG. Directory of solvents. London: Blackie; 1996. An imprint of Chapman & Hall; p. 14.